

Received: 2019.08.06

Accepted: 2019.10.28

Available online: 2020.01.21

Published: 2020.02.06

The Effects of RKI-1447 in a Mouse Model of Nonalcoholic Fatty Liver Disease Induced by a High-Fat Diet and in HepG2 Human Hepatocellular Carcinoma Cells Treated with Oleic Acid

Authors' Contribution:
Study Design A
Data Collection B
Statistical Analysis C
Data Interpretation D
Manuscript Preparation E
Literature Search F
Funds Collection G

ABCDEF **Jinshan Wang**
ABCDEFG **Wentao Jiang**

Department of Transplantation, Tianjin First Central Hospital, Tianjin, P.R. China

Corresponding Author: Wentao Jiang, e-mail: xy5577368@163.com

Source of support: This study was supported by The National Natural Science Foundation of China (Grant No. 81870444), the Tianjin Science and Technology Plan Project (Grant No. 17ZXMFSY00040), the Tianjin Science and Technology Plan Project (Grant No. 14RCGFSY00147), the International S&T Cooperation Program of China (Grant No. 2015DFG31850), and the National Key Clinical Specialty Construction Project of Organ Transplantation Department (Grant No. 2013544)

Background: This study aimed to investigate the effects of RKI-1447, a selective inhibitor of Rho-associated ROCK kinases, in a mouse model of nonalcoholic fatty liver disease (NAFLD) induced by a high-fat diet, and in oleic acid-treated HepG2 human hepatocellular carcinoma cells *in vitro*.





Material/Methods: Four study groups of mice included: the control group; the high-fat diet (HFD) group; the HFD+RKI-1447 (2 mg/kg) group; and the HFD+RKI-1447 (8 mg/kg) group. Mice were fed a high-fat diet for 12 weeks. Mice in the HFD+RKI-1447 groups were fed a high-fat diet for 12 weeks and treated with RKI-1447 twice weekly for three weeks. The HepG2 human hepatocellular carcinoma cells were treated with or without RKI-1447 for 2 h and treated with oleic acid for 24 h.

Results: In the mouse model of NAFLD, RKI-1447 reduced insulin resistance and the levels of alanine aminotransferase (ALT), aspartate transaminase (AST), total cholesterol, triglyceride, interleukin-6 (IL-6), tumor necrosis factor- α (TNF- α), malondialdehyde (MDA), and superoxide dismutase (SOD). RKI-1447 reduced the histological changes in the mouse model of NAFLD in mice fed a high-fat diet and significantly inhibited the generations of triglyceride, IL-6, and TNF- α . RKI-1447 reduced the levels of oxidative stress in HepG2 cells treated with oleic acid and significantly down-regulated the expression of RhoA, ROCK1, ROCK2, toll-like receptor 4 (TLR4), p-TBK1, and p-IRF3. RKI-1447 treatment also inhibited RhoA expression.

Conclusions: In a mouse model of NAFLD, RKI-1447 inhibited ROCK and modulated insulin resistance, oxidative stress, and inflammation through the ROCK/TLR4/TBK1/IRF3 pathway.

MeSH Keywords: **Diet, High-Fat • Liver Diseases • rho-Associated Kinases**

Full-text PDF: <https://www.medscimonit.com/abstract/index/idArt/919220>

 4440   14  39



Background

Nonalcoholic fatty liver disease (NAFLD) is a common and prevalent liver disease in industrialized countries and is a progressive condition of the liver that is associated with an increased sedentary lifestyle, obesity, and a high-fat diet. NAFLD is characterized by triglyceride accumulation in hepatocytes, nonalcoholic steatohepatitis (NASH), and lobular inflammation [1]. Some patients with NASH may develop cirrhosis and hepatocellular carcinoma (HCC). NAFLD can be associated with hypertension, insulin resistance, and dyslipidemia, and affects the quality of life of patients [2]. Although recent advances have been achieved in the diagnosis of NAFLD, the etiology remains poorly understood. Therefore, there is a need for further studies on the pathogenesis and treatment of NAFLD.

The occurrence of NAFLD is attributed to several factors, including disturbance of lipid metabolism, mitochondrial dysfunction, insulin resistance, oxidative stress, and inflammation [3]. Studies have supported that NAFLD involves metabolic dysregulation of fatty acid utilization and glucose metabolism, which contribute to increased oxidative effects and inflammation. A mouse model of NAFLD has been established that includes mice fed a high-fat diet, and this model results in obesity and insulin resistance. The development of NAFLD is believed to result from an imbalance between pro-inflammatory and anti-inflammatory phenomena [4,5].

RhoA is a small G-protein that binds to the plasma membrane. RhoA stimulation activates Rho-associated protein kinase 1 (ROCK1) and ROCK2, which are two isoforms that share 92% identity of kinase domains. ROCK1 and ROCK2 are involved in several cellular roles, including the cytoskeleton, cell migration, oxidative stress, lipid metabolism, and inflammation [6]. Toll-like receptor 4 (TLR4) was involved in RhoA/ROCK-mediated dysfunction in oxidative responses and inflammation [7]. As a prominent downstream modulator of TLR4, TANK-binding kinase 1 (TBK1) controls interferon regulatory factor 3 (IRF3), which controls the transcription and recruitment of inflammatory cytokines [8]. Increased expression of IRF3 triggers the development of inflammation. Also, IRF3 signaling was reported to promote inflammation of adipose tissue and insulin resistance [9]. A previous study showed that IRF3 activation accelerated hepatocyte inflammation and metabolic abnormalities in NAFLD [10].

Studies have also shown that RhoA/ROCK expression was involved in hepatic cirrhosis [11], hepatocellular carcinoma [12], and diabetes [13]. However, the mechanism of RhoA/ROCK in NAFLD remains unclear. RKI-1447 is a selective ROCK inhibitor that has shown anti-tumor properties [14]. However, there have been few studies to determine the pharmacological effect of RKI-1447 in hepatic disease, including NAFLD. Therefore, this study aimed to investigate the effects of RKI-1447, a selective

inhibitor of Rho-associated ROCK kinases, in a mouse model of NAFLD induced by a high-fat diet, and in oleic acid-treated HepG2 human hepatocellular carcinoma cells *in vitro*.

Material and Methods

Materials

The Rho-kinase inhibitor, RKI-1447 (CAS No. 1342278-01-6), was obtained from MedChemExpress (Monmouth Junction, NJ, USA). ACCU-CHEX blood glucose meters and test strip were supplied from Roche (Basel, Switzerland). Alanine transaminase (ALT), aspartate transaminase (AST), total cholesterol, triglyceride, malondialdehyde (MDA), and superoxide dismutase (SOD) were obtained from Nanjing Jiancheng Bioengineering Institute (Nanjing, China). Oleic acid was supplied by Sigma-Aldrich (St. Louis MO, USA). Interleukin-6 (IL-6), and tumor necrosis factor- α (TNF- α) enzyme-linked immunosorbent assay (ELISA) kits were obtained from Elabscience (Wuhan, Hubei, China). Dulbecco's modified Eagle's medium (DMEM) medium was provided by Gibco (Thermo Fisher Scientific, Waltham, MA, USA). The antibody to RhoA was purchased from Abcam (Cambridge, UK). Other antibodies were obtained from Cell Signaling Technology (Danvers, MA, USA).

The mouse model of nonalcoholic fatty liver disease (NAFLD) induced by a high-fat diet

Male Institute of Cancer Research (ICR) mice (age, 6–8 weeks) were purchased from Beijing Wei Tong Li Hua Laboratory Animal Technology Co., Ltd. and housed in standard conditions at 24–26°C, with a 12-hour light and dark cycle. The animals had free access to food and water. The animal experiments were conducted according to a protocol approved by the Animal Care and Ethics Committee of the First Central Hospital of Tianjin.

The high-fat diet and the regular mouse diet were obtained from Meidisen Biomedical Company (Jiangsu, China). The caloric content of the high-fat diet was composed of 20% carbohydrate, 20% protein, and 60% fat. The caloric content of the regular mouse diet was composed of 70% carbohydrate, 20% protein, and 10% fat.

The mouse study groups according to diet and treatment with and without RKI-1447

After seven days of acclimation, the mice were randomly assigned to four study groups: the control group; the high-fat diet (HFD) group; the HFD+RKI-1447 (2 mg/kg) group; and the HFD+RKI-1447 (8 mg/kg) group. The mice were fed with a high-fat diet for 12 weeks. The control mice were fed with a regular diet. From the ninth week, the mice in the

HFD+RKI-1447 (2 mg/kg) group and HFD+RKI-1447 (8 mg/kg) group were treated with intragastric RKI-1447 twice weekly for three weeks. The RKI-1447 was dissolved in dimethyl sulfoxide (DMSO) and normal saline with a concentration of DMSO <0.1% (v/v). The control mice and the mice in the high-fat diet group were given the vehicle orally.

Following an oral glucose tolerance test (OGTT) and insulin tolerance test (ITT), the mice were euthanized, and blood samples were harvested. The blood was centrifuged at 2,000×g, and the serum was stored at –80°C for further tests. The liver tissues were immediately removed on ice, and some samples were fixed in 4% paraformaldehyde solution, and other samples were stored at –80°C for biochemical tests and Western blot analysis.

Oral glucose tolerance test (OGTT)

The OGTT was performed after the last week of treatment to evaluate glucose tolerance. The mice fasted overnight and were then injected with 2 g/kg of glucose solution. Blood glucose (BG) levels were measured at 0, 30, 60, and 120 min. The area under the curve (AUC) was calculated according to the following formula:

$$\text{AUC} = 0.25 \times \text{BG} (0 \text{ min}) + 0.5 \times \text{BG} (30 \text{ min}) + 0.75 \times \text{BG} (60 \text{ min}) + 0.5 \times \text{BG} (120 \text{ min})$$

Insulin tolerance test (ITT)

After an overnight fast, the mice were injected intraperitoneally with 0.75 U/kg of Humulin R insulin (Eli Lilly, Kobe, Japan). Blood was sampled at 0, 30, 60, and 120 min post-injection. The AUC was calculated using the following formula:

$$\text{AUC} = 0.25 \times \text{BG} (0 \text{ min}) + 0.5 \times \text{BG} (30 \text{ min}) + 0.75 \times \text{BG} (60 \text{ min}) + 0.5 \times \text{BG} (120 \text{ min})$$

Culture of HepG2 human hepatocellular carcinoma cells and treatment with oleic acid (OA) and RKI-1447

HepG2 human hepatocellular carcinoma cells were obtained from the American Type Culture Collection (ATCC) (Manassas, VA, USA) were cultured with high-glucose Dulbecco's modified Eagle's medium (DMEM) supplemented with 10% fetal bovine serum (Hyclone, Logan, UT, USA), 100 IU/ml penicillin and 100 IU/ml streptomycin (Amresco, Solon, OH, USA) in an atmosphere of 5% CO₂ at 37°C.

The HepG2 cells were seeded at a density of 2×10⁵ cells/ml. The cells were divided into five groups: the control group; the oleic acid (OA) group; the OA+RKI-1447 (200 nM) group; the OA+RKI-1447 (400 nM) group; and the OA+RKI-1447 (800 nM)

group. Then, 24 h later, the cells were treated with or without RKI-1447 for 2 h, followed by 100 μM oleic acid dissolved in bovine serum albumin (BSA) solution. The control group was treated with BSA at the same volume. After further culture for 24 h, the cells were collected for further study.

MTT assay

The five groups of HepG2 cells were cultured in medium containing 0.5 mg/ml of MTT solution. After 4 h, the supernatant was removed, and the cells were treated with 150 μl of dimethyl sulfoxide (DMSO). The results were recorded at 540 nm with a microplate spectrophotometer.

Measurement of the biochemical indices of oxidative stress

The fresh hepatic tissue from each mouse was homogenized on ice using ice-cold normal saline and then centrifuged at 10,000×g for 20 min. The supernatants were carefully harvested and stored at –80°C. The levels of alanine aminotransferase (ALT), aspartate transaminase (AST), total cholesterol, and triglyceride in the serum, and malondialdehyde (MDA), and superoxide dismutase (SOD) in the serum and liver tissues were measured according to the instructions of manufacturers of the commercial kits (Nanjing Jiancheng Bio-engineering Institute, Nanjing, China). Levels of triglyceride, MDA, and SOD were measured in the cell supernatants.

Measurement of inflammatory cytokines

The levels of interleukin-6 (IL-6), tumor necrosis factor-α (TNF-α), in liver homogenate, serum, and culture supernatants were measured with the commercial ELISA kits, in accordance with the manufacturer's instructions.

Histology

The liver tissues were removed and fixed with 4% paraformaldehyde solution. The samples were dehydrated in ethanol, embedded in paraffin wax, and sectioned at 5 μm in thickness onto glass slides. Tissue sections were stained with hematoxylin and eosin (H&E). The liver histology was reviewed by two trained investigators who were blinded to the experimental design and study groups.

Immunohistochemistry

The fixed mouse liver tissue sections were examined for RhoA expression using immunohistochemistry. The tissue sections were heated for 1 h, deparaffinized using xylene, and rehydrated in graded ethanol solution, and microwaved in sodium citrate for antigen retrieval. Tissue sections were incubated

with 3% fresh hydrogen peroxide and blocked with 3% BSA at 25°C. After incubating with anti-RhoA primary antibody at 4°C overnight, the sections were treated with secondary antibodies at 37°C for 20 min. The samples were counterstained with 3,3-diaminobenzidine (DAB) and hematoxylin solution in the dark. The tissue sections were dehydrated and visualized using light microscopy. The liver immunohistochemistry was reviewed by two trained investigators who were blinded to the experimental design and study groups.

Confocal immunofluorescence

The HepG2 cells were seeded in a six-well plate and fixed with 4% paraformaldehyde, rehydrated, and then treated with 0.2% Triton X-100 for 5 min. The cells were blocked with 2% BSA. After washing with PBS, the HepG2 cells were treated with primary antibodies overnight. The cells were incubated with Alexa Fluor 594-conjugated secondary antibodies at room temperature, and further stained with 4,6-diamidino-2-phenylindole (DAPI) solution for approximate 15 min before examination with a confocal laser scanning microscope (Olympus, Shinjuku, Tokyo, Japan). The confocal immunofluorescence staining images were reviewed by two trained investigators who were blinded to the experimental design and study groups.

Western blot

The hepatic tissue and cell homogenate were lysed in RIPA buffer (Beyotime, Shanghai, China). The samples were then centrifuged at 12,000 x g for 5 min on ice, and the supernatant was collected. The protein content was measured using a BCA detection kit (Beyotime, Shanghai, China). The protein samples were separated by 8–12% sodium dodecyl sulfate-polyacrylamide gel electrophoresis (SDS-PAGE) and transferred onto polyvinylidene difluoride (PVDF) membranes (Merck Millipore, Burlington, MA, USA). The membranes were washed, blocked with 5% dried skimmed milk powder dissolved in TBS containing 0.1% Tween-20 (TBST) for 1 h at room temperature. The blots were incubated with the primary antibodies. The membranes were then washed three times in TBST and incubated with the appropriate horseradish peroxidase (HRP)-labeled secondary antibody for 1 h at room temperature. After washing three times in TBST, the detection was performed using electrochemiluminescence (ECL) and a microplate reader. The images were quantified using ImageJ software (National Institutes of Health, Bethesda, MD, USA).

Statistical analysis

The results were presented as the mean±standard deviation (SD). Statistically significant differences were calculated using one-way analysis of variance (ANOVA) with Tukey's multiple comparison test and analyzed with GraphPad version 5.0

software (GraphPad Software, La Jolla, CA, USA). A P-value <0.05 was considered to be statistically significant.

Results

The effects of RKI-1447 on glucose tolerance and insulin resistance in the mouse model of nonalcoholic fatty liver disease (NAFLD) induced by a high-fat diet

The mouse model of nonalcoholic fatty liver disease (NAFLD) induced by a high-fat diet,

and treated with or without RKI-1447 were divided into four study groups: the control group; the high-fat diet (HFD) group; the HFD+RKI-1447 (2 mg/kg) group; and the HFD+RKI-1447 (8 mg/kg) group. Glucose challenge resulted in a significant increase in blood glucose in each group. The glucose concentration in all the groups reached a peak at 30 min, and then gradually decreased. By 120 min after glucose treatment, the HFD group remained hyperglycemic when compared with the control group. Treatment with RKI-1447 significantly reduced the blood glucose level compared with the HFD group. The area under the curve (AUC) of the HFD group was significantly greater than that in the control group ($p<0.05$), while the RKI-1447 (8 mg/kg) group had a significantly reduced the AUC value ($p<0.05$).

Insulin resistance is considered to be a reliable method of evaluating glucose homeostasis in NAFLD. The glucose levels in the HFD group were significantly higher than those in the control group. Treatment with RKI-1447 (8 mg/kg) significantly decreased blood glucose at 0 min, 60 min, and 120 min. The significantly higher AUC was confirmed in the HFD group when compared with the control group ($p<0.01$), whereas the RKI-1447 (2 mg/kg to 8 mg/kg) treatment effectively decreased the AUC ($p<0.05$).

The protein expression of the insulin receptor substrate-1 (IRS-1), a critical biomarker of insulin resistance, was also measured. The HFD challenge reduced the phosphorylation of IRS1 compared with the control group ($p<0.05$), while the RKI-1447 (2 mg/kg to 8 mg/kg) group increased the p-IRS1 levels ($p<0.05$). The study findings showed that RKI-1447 significantly improved glucose tolerance and insulin resistance (Figure 1).

The effects of RKI-1447 on the serum transaminase levels in the mouse model of NAFLD

The ALT and AST activities were determined to reflect hepatocellular injury. As illustrated in Figure 2, the results indicate that the high-fat diet in the mouse model of NAFLD resulted in a significant increase in the serum levels of ALT and AST ($p<0.001$). Treatment with ROCK inhibitor RKI-1447 (2 mg/kg)

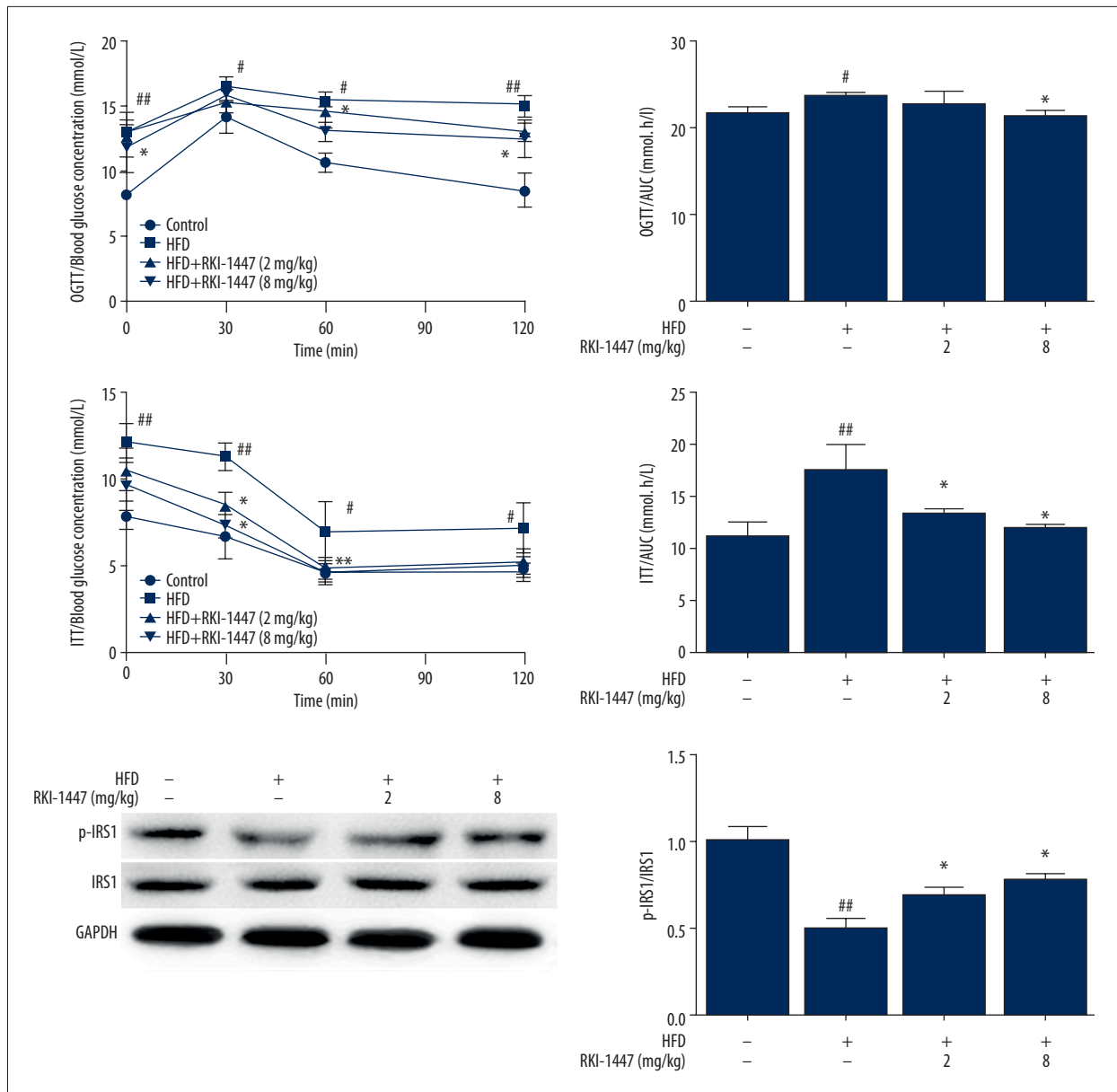


Figure 1. The effects of RKI-1447 on glucose tolerance and insulin resistance in a mouse model of nonalcoholic fatty liver disease (NAFLD) induced by a high-fat diet. The blood glucose and area under the curve (AUC) for the oral glucose tolerance test (OGTT), the blood glucose and AUC for the insulin tolerance test (ITT), and the expression of the insulin receptor substrate-1 (IRS1) are shown. The mice were fed with a high-fat diet for 12 weeks. From the ninth week, the mice were treated orally with the ROCK inhibitor RKI-1447 (2 mg/kg to 8 mg/kg) twice weekly for three weeks. Data are expressed as the mean±SD. Compared with the control: ## p<0.01, ### p<0.001. Compared with a high-fat diet: * p<0.05, ** p<0.01, *** p<0.001.

and RKI-1447 (8 mg/kg) contributed to the significant reduction in ALT level (p<0.05, p<0.001, respectively). RKI-1447 (8 mg/kg) also significantly reduced the ALT level compared with the HFD group (p<0.01), which was greater than the RKI-1447 (2 mg/kg) group (p<0.05). These results indicated that the inhibition of ROCK significantly reduced the activity of transaminases.

The effects of RKI-1447 on hepatic lipid in the mouse model of NAFLD

The concentrations of total cholesterol and triglyceride were monitored in serum to determine the effect of RKI-1447 on lipid metabolism. As shown in Figure 3, total cholesterol and triglyceride were significantly increased in the HFD group compared with the control group (p<0.01). Injection of RKI-1447(8 mg/kg)

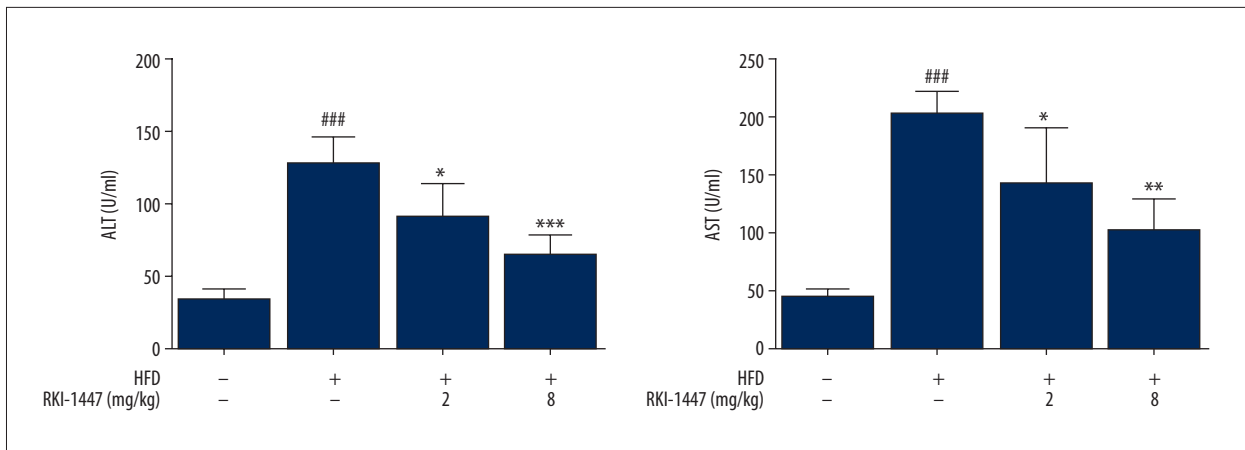


Figure 2. RKI-1447 reduced the serum levels of alanine aminotransferase (ALT) and aspartate transaminase (AST) in a mouse model of nonalcoholic fatty liver disease (NAFLD) induced by a high-fat diet. The mice were fed a high-fat diet for 12 weeks. From the ninth week, the mice were treated orally with the ROCK inhibitor RKI-1447 (2 mg/kg to 8 mg/kg) twice weekly for three weeks. Data are expressed as the mean±SD. Compared with the control: ## $p<0.01$, ### $p<0.001$. Compared with a high-fat diet: * $p<0.05$, ** $p<0.01$, *** $p<0.001$.

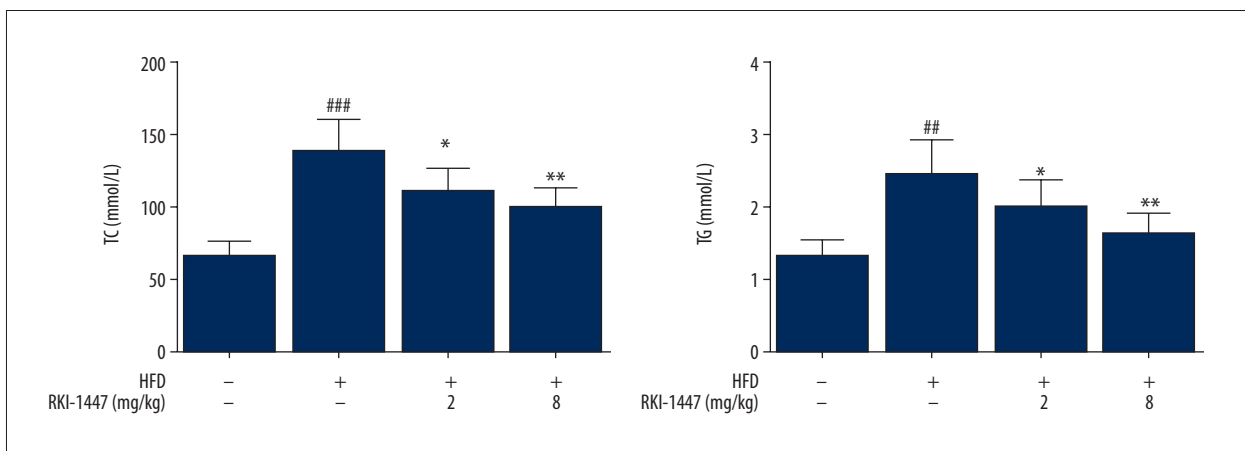


Figure 3. The effects of RKI-1447 on the serum levels of total cholesterol and triglyceride in a mouse model of nonalcoholic fatty liver disease (NAFLD) induced by a high-fat diet. The mice were fed a high-fat diet for 12 weeks. From the ninth week, the mice were treated orally with the ROCK inhibitor RKI-1447 (2 mg/kg to 8 mg/kg) twice weekly for three weeks. Data are expressed as the mean±SD. Compared with the control: ## $p<0.01$, ### $p<0.001$. Compared with a high-fat diet: * $p<0.05$, ** $p<0.01$.

significantly reduced the total cholesterol level compared with the HFD group ($p<0.01$), which was more effective than the RKI-1447 (8 mg/kg) group ($p<0.05$). RKI-1447 (8 mg/kg) also reduced the triglyceride content ($p<0.01$). These findings showed that the inhibition of ROCK reduced the degree of changes associated with NAFLD in the mouse model.

The effects of RKI-1447 on inflammatory cytokines in serum and in liver tissues in the mouse model of NAFLD

As shown in Figure 4, a high-fat diet in the mouse model significantly increased the levels of IL-6 and TNF- α in the serum. RKI-1447 (2 mg/kg to 8 mg/kg) significantly reduced the levels of IL-6 ($p<0.05$, $p<0.01$, respectively). RKI-1447 (8 mg/kg)

treatment also significantly down-regulated TNF- α expression ($p<0.05$).

The high-fat diet used in the mouse model of NAFLD was associated with increased levels of IL-6 and TNF- α in liver tissues ($p<0.01$, $p<0.05$, respectively). IL-6 levels were reduced by RKI-1447 (8 mg/kg) when compared with the HFD group ($p<0.01$). In the RKI-1447 (8 mg/kg) group, there were significantly reduced TNF- α levels compared with the HFD group ($p<0.05$). Inhibition of ROCK reduced the expression levels of serum and liver inflammatory cytokines in HFD-induced NAFLD in the mouse model.

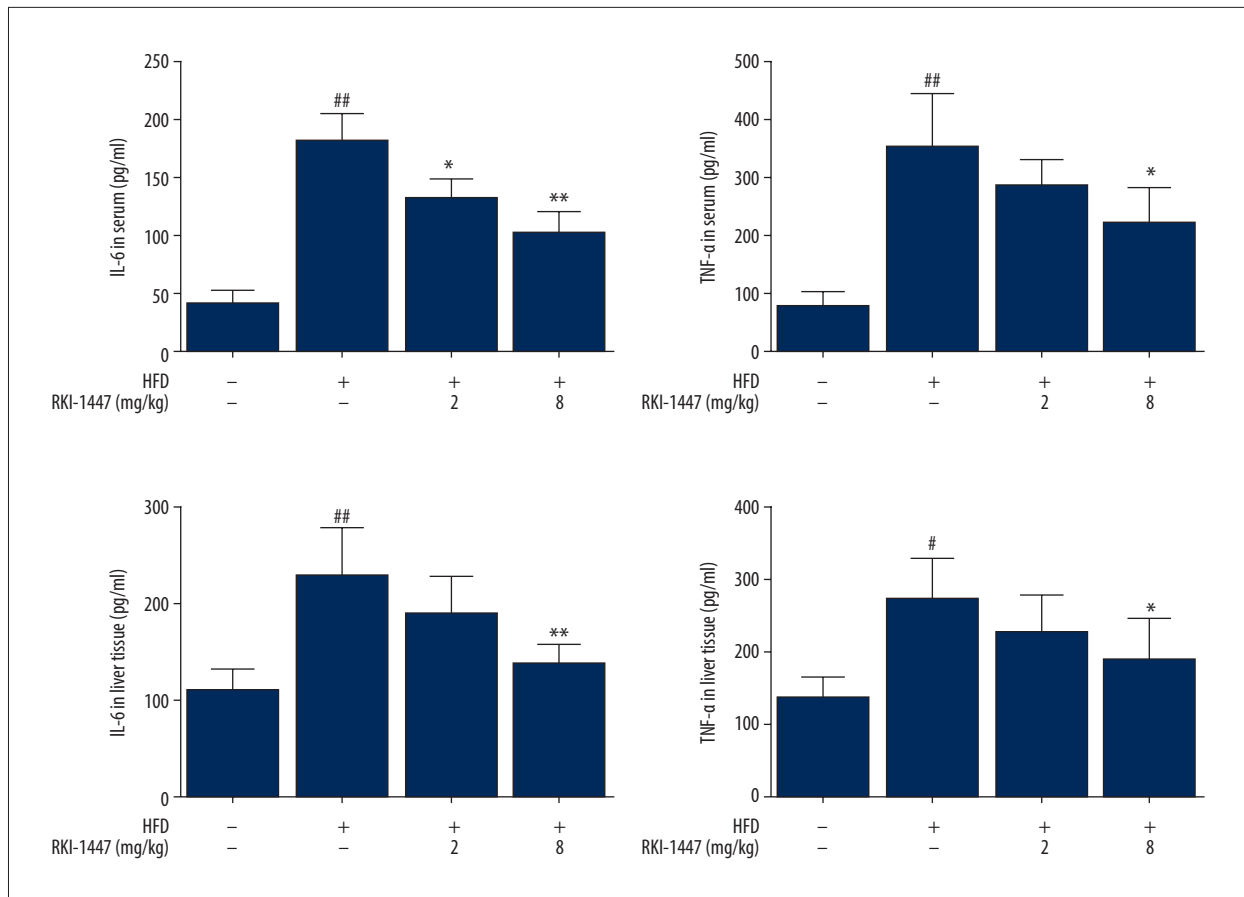


Figure 4. The effects of RKI-1447 on the levels of interleukin-6 (IL-6) and tumor necrosis factor- α (TNF- α) in serum and liver tissues in a mouse model of nonalcoholic fatty liver disease (NAFLD) induced by a high-fat diet. The mice were fed a high-fat diet for 12 weeks. From the ninth week, the mice were treated orally with the ROCK inhibitor RKI-1447 (2 mg/kg to 8 mg/kg) twice weekly for three weeks. Data are expressed as the mean \pm SD. Compared with the control: ## $p < 0.01$, ### $p < 0.001$. Compared with a high-fat diet: * $p < 0.05$, ** $p < 0.01$.

The effects of RKI-1447 on malondialdehyde (MDA) and superoxide dismutase (SOD) levels in serum and hepatic tissues in the mouse model of NAFLD

As shown in Figure 5, the HFD group showed a significant increase in serum levels of MDA and a decrease of serum SOD levels compared with the control group ($p < 0.01$). RKI-1447 (8 mg/kg) significantly reduced the serum level of MDA ($p < 0.05$). RKI-1447 (2 mg/kg to 8 mg/kg) treatment groups showed significantly increased activity of SOD ($p < 0.05$, $p < 0.01$) compared with the HFD group.

The effects of RKI-1447 on the liver histology in the mouse model of NAFLD

Figure 6 shows the appearance of the liver histology in mice fed a high-fat diet. The liver in the mouse model of NAFLD showed the characteristic changes of steatosis with lipid droplets within the hepatocytes, and an interstitial inflammatory

cell infiltrate. RKI-1447 treatment significantly reduced the severity of the histological changes. The RKI-1447 (8 mg/kg) and RKI-1447 (2 mg/kg) groups showed less hepatic steatosis, and inflammatory cell infiltrates. These results supported that the inhibition of ROCK reduced the histopathological changes induced by a high-fat diet in the mouse model of NAFLD.

The effects of RKI-1447 on the immunohistochemistry for RhoA expression in liver tissues in the mouse model of NAFLD

The hepatic expression of RhoA was studied by immunohistochemistry in the mouse liver tissues. As shown in Figure 7, there were few immunopositive cells in the control group. The expression of RhoA was increased in the mouse model of NAFLD given a high-fat diet. RhoA expression was reduced following treatment with RKI-1447 (2 mg/kg) and RKI-1447 (8 mg/kg).

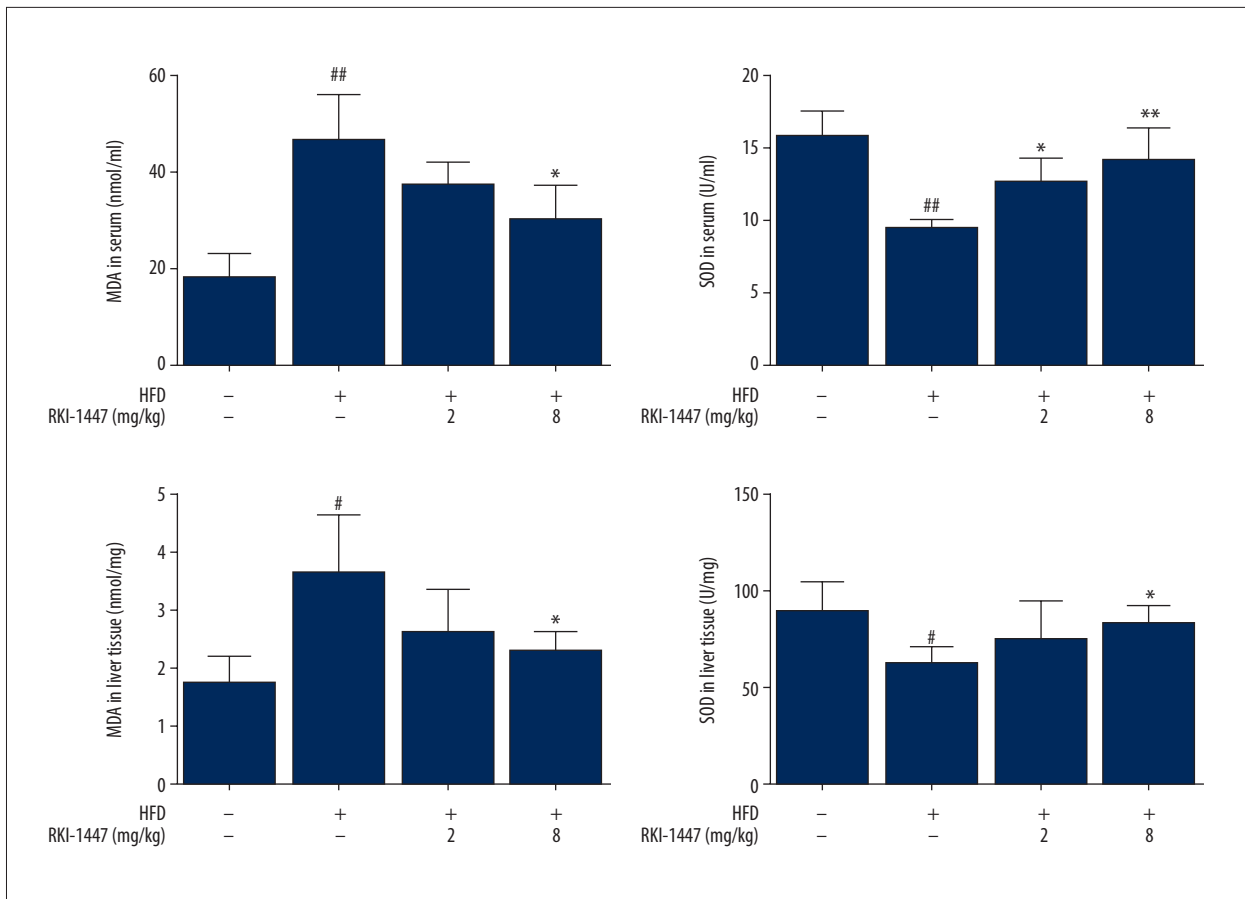


Figure 5. The effects of RKI-1447 on the levels of malondialdehyde (MDA) and superoxide dismutase (SOD) in serum and hepatic tissues in a mouse model of nonalcoholic fatty liver disease (NAFLD) induced by a high-fat diet. The mice were fed a high-fat diet for 12 weeks. From the ninth week, the mice were treated orally with the ROCK inhibitor RKI-1447 (2 mg/kg to 8 mg/kg) twice weekly for three weeks. Data are expressed as the mean±SD. Compared with the control: ^{##} $p < 0.01$, ^{###} $p < 0.001$. Compared with mice fed a high-fat diet: ^{*} $p < 0.05$, ^{**} $p < 0.01$.

The effects of RKI-1447 on the ROCK/TLR4/TBK1/IRF3 pathway in hepatic tissues in the mouse model of NAFLD

In the mouse model of NAFLD given a high-fat diet overexpression of RhoA, ROCK1, ROCK2, TLR4, p-TBK1, and p-IRF3 were found ($p < 0.05$, or $p < 0.01$). However, inhibition of ROCK by RKI-1447 (8 mg/kg) significantly inhibited the expression of RhoA, ROCK1, and TLR4 ($p < 0.01$) when compared with the HFD group, and this difference was more significant than for the RKI-1447 (2 mg/kg) group ($p < 0.05$). Also, RKI-1447 (8 mg/kg) also significantly down-regulated the expression of ROCK2, p-TBK1, and p-IRF3 ($p < 0.05$). (Figure 8)

The effects of RKI-1447 on the cytotoxicity and the triglyceride content in oleic acid-treated HepG2 cells

HepG2 cells were divided into five study groups: the control group; the oleic acid (OA) group; the OA+RKI-1447 (200 nM) group; the OA+RKI-1447 (400 nM) group; and the

OA+RKI-1447 (800 nM) group. HepG2 cells were used to investigate the underlying molecular mechanism of the ROCK inhibitor RKI-1447 on NAFLD *in vitro*. Oleic acid significantly induced hepatocyte intracellular lipid accumulation ($p < 0.001$). Oleic acid stimulation, RKI-1447 (200 nM, 400 nM, and 800 nM) did not significantly affect cell viability. The effect of oleic acid (OA) and RKI-1447 (200 nM, 400 nM, and 800 nM) did not result in cytotoxicity in HepG2 cells. RKI-1447 (800 nM) significantly reduced the triglyceride content when compared with the OA group ($p < 0.01$), which was more significantly reduced than the RKI-1447 (400 nM) group ($p < 0.05$). (Figure 9)

The effects of RKI-1447 on the inflammatory cytokines in oleic acid-treated HepG2 cells

Concentrations of IL-6 and TNF- α in the cell culture supernatant were investigated to evaluate the anti-inflammatory activities of RKI-1447 *in vitro*. As shown in Figure 10, the levels of IL-6 and TNF- α in the culture supernatant were significantly

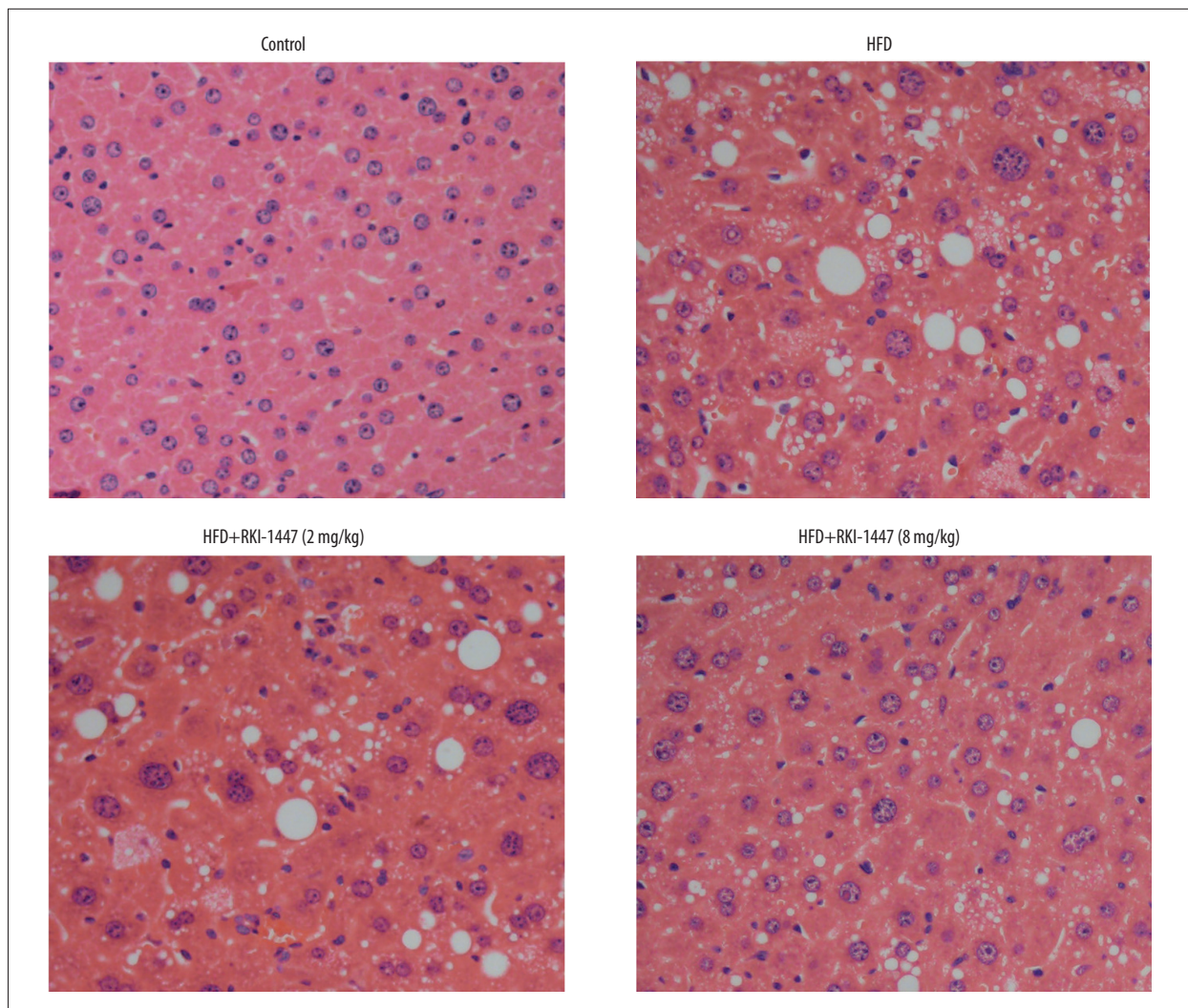


Figure 6. The effects of RKI-1447 on the liver histology in a mouse model of nonalcoholic fatty liver disease (NAFLD) induced by a high-fat diet. The mice were fed a high-fat diet for 12 weeks. From the ninth week, the mice were treated orally with the ROCK inhibitor RKI-1447 (2 mg/kg to 8 mg/kg) twice weekly for three weeks.

increased ($p < 0.01$). Treatment with RKI-1447 (800 nM) significantly reduced the IL-6 and TNF- α levels ($p < 0.01$). Pre-treatment with RKI-1447 (400 nM) also significantly reduced the levels of IL-6 and TNF- α ($p < 0.05$). These results suggested that RKI-1447, an inhibitor of ROCK, blocked the synthesis and secretion of inflammatory cytokines from HepG2 cells *in vitro*.

The effects of RKI-1447 on oxidative stress in oleic acid-treated HepG2 cells

The levels of SOD and MDA were also determined *in vitro*. As shown in Figure 11, OA stimulation resulted in significantly reduced SOD activity and increased MDA levels ($p < 0.01$). However, the administration of RKI-1447 (400 nM and 800 nM) significantly reduced the MDA levels ($p < 0.05$). Also, RKI-1447 (800 nM) significantly increased SOD when compared with that of oleic

acid stimulation ($p < 0.01$), which was slightly more significant than that for the RKI-1447 (400 nM) group ($p < 0.05$).

The effects of RKI-1447 on the expression of RhoA in oleic acid-treated HepG2 cells shown by confocal immunofluorescence

Confocal immunofluorescence microscopy was used to visualize the cellular location of RhoA in oleic acid-treated HepG2 cells. As shown in Figure 12, the immunolocalization of RhoA was increased by the oleic acid challenge. However, RKI-1447 (200 nM, 400 nM, and 800 nM) inhibited RhoA expression in a concentration-dependent manner. These findings supported that RKI-1447 treatment inhibited RhoA expression levels in OA-induced HepG2 cells *in vitro*.

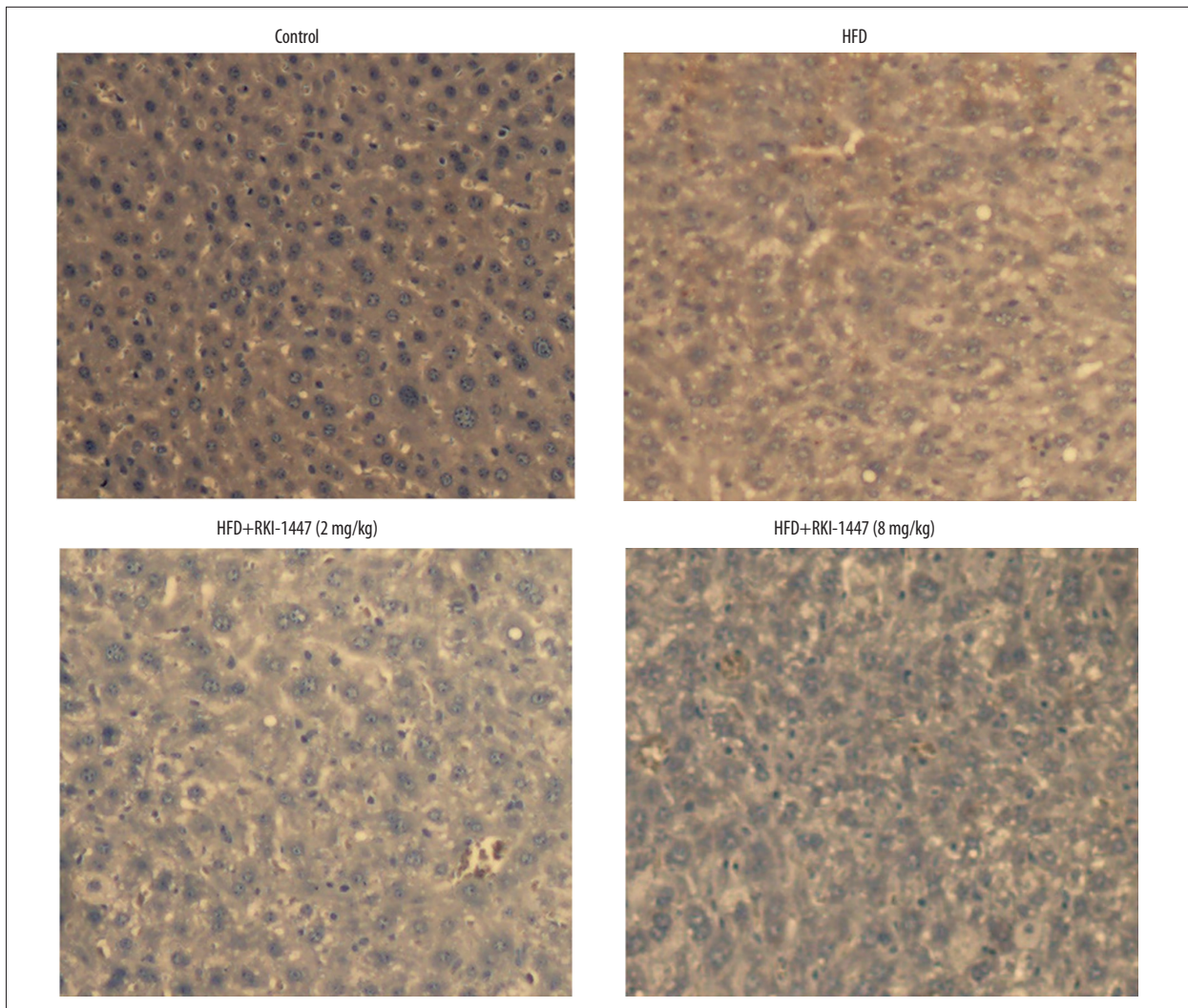


Figure 7. The effects of RKI-1447 on the immunohistochemistry for RhoA expression in liver tissues in a mouse model of nonalcoholic fatty liver disease (NAFLD) induced by a high-fat diet. The mice were fed a high-fat diet for 12 weeks. From the ninth week, the mice were treated orally with the ROCK inhibitor RKI-1447 (2 mg/kg to 8 mg/kg) twice weekly for three weeks. Data are expressed as the mean \pm SD. Compared with the control: ## $p<0.01$, ### $p<0.001$. Compared with mice fed a high-fat diet: * $p<0.05$, ** $p<0.01$.

The effects of RKI-1447 on the expression of proteins in the ROCK/TLR4/TBK1/IRF3 pathway in oleic acid-treated HepG2 cells

The protein expression levels of RhoA, TLR4, p-TBK1, TBK1, p-IRF3, IRF3 were studied in HepG2 cells. As shown in Figure 10, the expression of RhoA, TLR4, p-TBK1, and p-IRF3 were upregulated. However, treatment with RKI-1447 (800 nM) significantly down-regulated the expression of RhoA ($p<0.01$). RKI-1447 (200 nM and 400 nM) also had a similar effect ($p<0.05$). The data indicated that RKI-1447 significantly inhibited ROCK signaling in the oleic acid-treated HepG2 cells. Treatment with RKI-1447 (400 nM and 800 nM) significantly inhibited the protein levels of TLR4, p-TBK1 ($p<0.05$). RKI-1447 (400 nM and

800 nM) also significantly reduced the phosphorylation of p-IRF3 ($p<0.01$, $p<0.01$, respectively). These results demonstrated that the inhibition of ROCK by RKI-1447 resulted in suppression of ROCK/TLR4/TBK1/IRF3 pathway in HepG2 cells *in vitro* (Figure 13).

Discussion

Nonalcoholic fatty liver disease (NAFLD) is associated with a range of changes in the liver cells and liver parenchyma that include mitochondrial dysfunction, lipid peroxidation, and inflammation that contribute to the progression of NAFLD. Abnormal lipid metabolism remains the major cause of NAFLD [15]. Excess

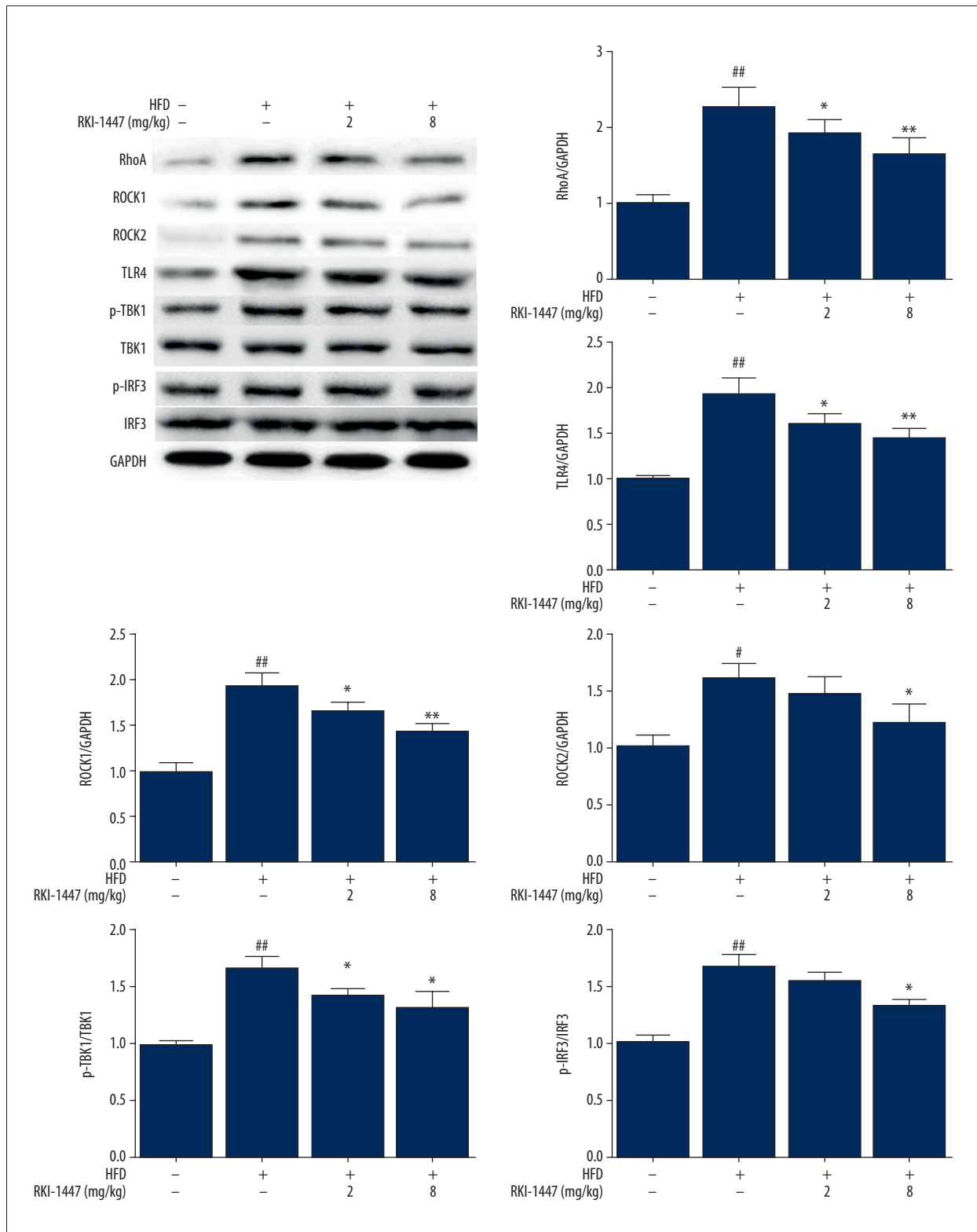


Figure 8. The effects of RKI-1447 on the ROCK/TLR4/TBK1/IRF3 pathway in hepatic tissues in a mouse model of nonalcoholic fatty liver disease (NAFLD) induced by a high-fat diet. The mice were fed a high-fat diet for 12 weeks. From the ninth week, the mice were treated orally with the ROCK inhibitor RKI-1447 (2 mg/kg to 8 mg/kg) twice weekly for three weeks. Data are expressed as the mean±SD. Compared with the control: ^{##} p<0.01. Compared with mice fed a high-fat diet: ^{*} p<0.05, ^{**} p<0.01.

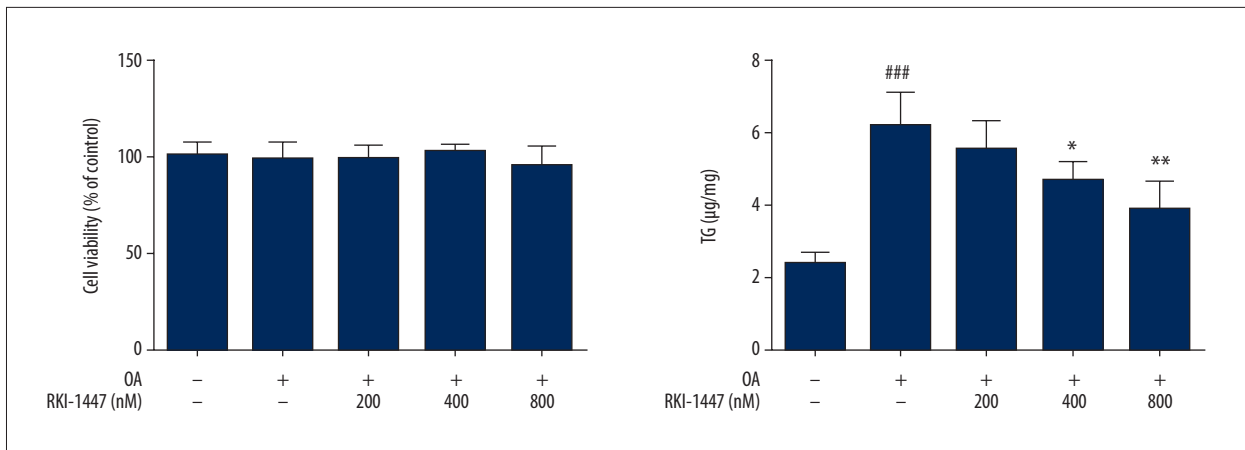


Figure 9. The effects of RKI-1447 on the triglyceride content in oleic acid-treated HepG2 human hepatocellular carcinoma cells. HepG2 cells were treated with or without the ROCK inhibitor RKI-1447 (200 nM, 400 nM, 800 nM) for 2 h. The cells were treated with oleic acid for 24 h and harvested. Data are expressed as the mean±SD. Compared with the control: ## $p<0.01$, ### $p<0.00$. Compared with mice fed a high-fat diet: * $p<0.05$, ** $p<0.01$.

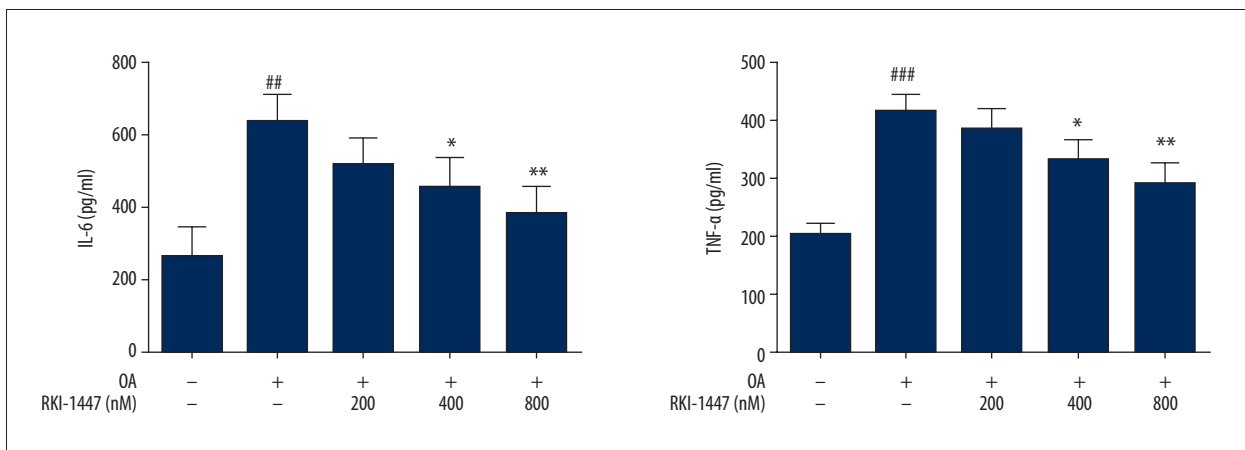


Figure 10. The effects of RKI-1447 on the levels of interleukin-6 (IL-6) and tumor necrosis factor- α (TNF- α) in the supernatant of oleic acid-treated HepG2 human hepatocellular carcinoma cells. HepG2 cells were treated with or without the ROCK inhibitor RKI-1447 (200 nM, 400 nM, 800 nM) for 2 h. The cells were treated with oleic acid for 24 h and harvested. Data are expressed as the mean±SD. Compared with the control: ## $p<0.01$, ### $p<0.00$. Compared with mice fed a high-fat diet: * $p<0.05$, ** $p<0.01$.

fat absorption from dietary intake directly leads to hepatic lipid generation and inflammation. NAFLD can be a hepatic manifestation of obesity and metabolic syndrome and is characterized by metabolic changes, increased serum triglyceride, hepatic steatosis, insulin resistance, oxidative stress, and chronic inflammation [16]. Oleic acid is a mono-unsaturated fatty acid that is present in the diet. Oleic acid has been shown to lead to cell apoptosis, autophagy, and inflammation, and its use in human HepG2 hepatocellular carcinoma cells and in a mouse model using a high-fat diet have previously been described as *in vitro* and *in vivo* models of NAFLD [17]. The measurement of serum levels of alanine aminotransferase (ALT) and aspartate transaminase (AST) are sensitive biomarkers for hepatic injury [18]. Lipid homeostasis is controlled by the balance between lipid

consumption and synthesis [19]. Excess intracellular lipid promotes mitochondrial damage, leading to dysfunction of energy metabolism and the transcription of inflammatory cytokines in liver tissues, and total cholesterol and triglyceride function as the reliable indicators for lipid accumulation [20].

The findings from the present study showed that mice fed with a high-fat diet showed increased levels of serum transaminases and increased triglyceride levels with and typical histological features of NAFLD. In this study, in a mouse model of NAFLD, RKI-1447 inhibited Rho-associated protein kinase (ROCK) and modulated insulin resistance, oxidative stress, and inflammation through the ROCK/TLR4/TBK1/IRF3 pathway. Also, HepG2 human hepatocellular carcinoma cells studied *in vitro* showed

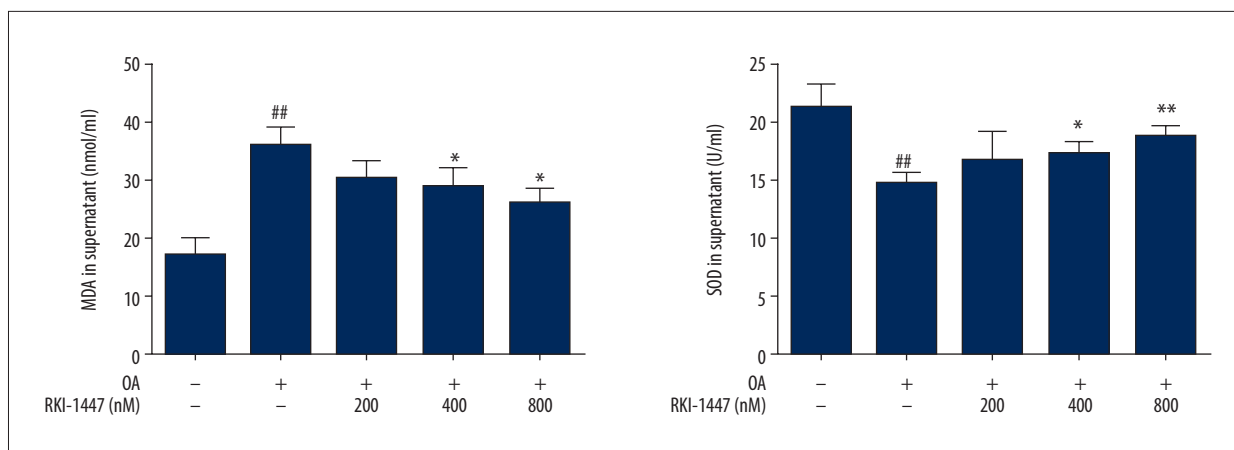


Figure 11. The effects of RKI-1447 on the levels of malondialdehyde (MDA) and superoxide dismutase (SOD) in the supernatant of oleic acid-treated HepG2 human hepatocellular carcinoma cells. HepG2 cells were treated with or without the ROCK inhibitor RKI-1447 (200 nM, 400 nM, 800 nM) for 2 h. The cells were treated with oleic acid for 24 h and harvested. Data are expressed as the mean±SD. Compared with the control: ^{##} p<0.01, ^{###} p<0.00. Compared with mice fed a high-fat diet: ^{*} p<0.05, ^{**} p<0.01.

that the inhibition of ROCK by RKI-1447, reduced the production of triglyceride caused by oleic acid treatment. These results demonstrated that the suppression of ROCK reduced the changes of NAFLD induced by a high-fat diet in the mouse model.

Insulin resistance is a clinical characteristic of NAFLD. Impaired insulin signaling is part of a molecular cascade that includes the insulin receptor substrate (IRS). Chronic low-grade inflammation and oxidative stress are accompanied by insulin resistance in NAFLD [21]. The results of the present study showed that treatment with RKI-1447 reduced insulin resistance and IRS phosphorylation. Chronic accumulation of triglyceride in the cytoplasm of hepatocytes results in hepatocellular injury, inflammation, and increased levels of reactive oxygen species (ROS), which contribute to NAFLD. Inflammation and oxidative stress are important factors in the etiology of nonalcoholic steatohepatitis (NASH) [22]. However, the development of NAFLD requires an inflammatory cellular environment that includes increased expression of IL-6 and TNF- α . IL-6 is a classical inflammatory cytokine that is involved in the pathogenesis of NAFLD, and TNF- α participates in the host immune response [23]. Treatment with a Rho kinase inhibitor reduced hypercholesterolemia and increased oxidative biomarkers [24]. The findings from the present study showed that a high-fat diet or oleic acid stimulated the upregulation of inflammatory cytokines and indices of oxidative stress, which were significantly reduced by the inhibitions of ROCK using RKI-1447.

The Rho-associated serine kinases modulate several pathological conditions, including lipid metabolism, oxidative stress, and inflammation [25]. Soliman et al. showed that the partial deletion of the ROCK2 gene reduced insulin resistance in transgenic mice fed a high-fat diet [26]. Studies have shown that the

activation of the RhoA/ROCK pathway was a potential target for hepatic inflammation [27]. Rho-kinases are overexpressed in hepatocellular carcinoma (HCC) [28]. ROCK has been proposed to control the levels of aminotransferase, total cholesterol, triglyceride, and inflammatory cytokines in STZ liver injury [29]. The findings from the present study also showed that following treatment with RKI-1447, the expression of RhoA were significantly inhibited. The protein levels of ROCK1 and ROCK2 were also reduced. These results showed the inhibition of ROCK in NAFLD induced by a high-fat diet and in HepG2 cells treated with oleic acid, and further confirmed that ROCK suppression had beneficial effects in NAFLD *in vivo* and *in vitro*.

The activation of the RhoA/ROCK pathway and TLR4 increase hepatocellular damage [30]. ROCK inhibitors also suppress TLR4 signaling [31]. It was previously reported that the RhoA/ROCK pathway governed TLR4/NF- κ B signaling and accelerated inflammation [32]. Previous studies have shown that ROCK1 was the upstream mediator of TLR4 in macrophages during liver fibrosis [33]. With the use of the ROCK inhibitor, Y-27632, Hutchinson et al. showed that the inflammatory cascade activated TLR4 signaling through ROCK [34]. Following the expression of TLR4, several transcription factors, including IFN regulatory factors (IRFs), are upregulated in alcoholic hepatic injury [35]. IRFs contain nine members (IRF-1 to IRF-9) [35]. As a downstream factor in TLR4 expression, TBK1 serves as the crucial regulator for IRF3 [36]. The phosphorylation of TBK1/IRF3 inhibits the inflammatory response in hepatitis [37]. IRF3 relieves hepatic steatosis and insulin resistance in high fat diet-induced metabolic dysfunction [38]. Previous studies have shown that IRF3 was involved in the reduction in levels of MDA and SOD [39]. Tsukamoto et al. proposed that the TLR4/TBK1/IRF3 signaling pathway mediated the inflammatory response to LPS [8].

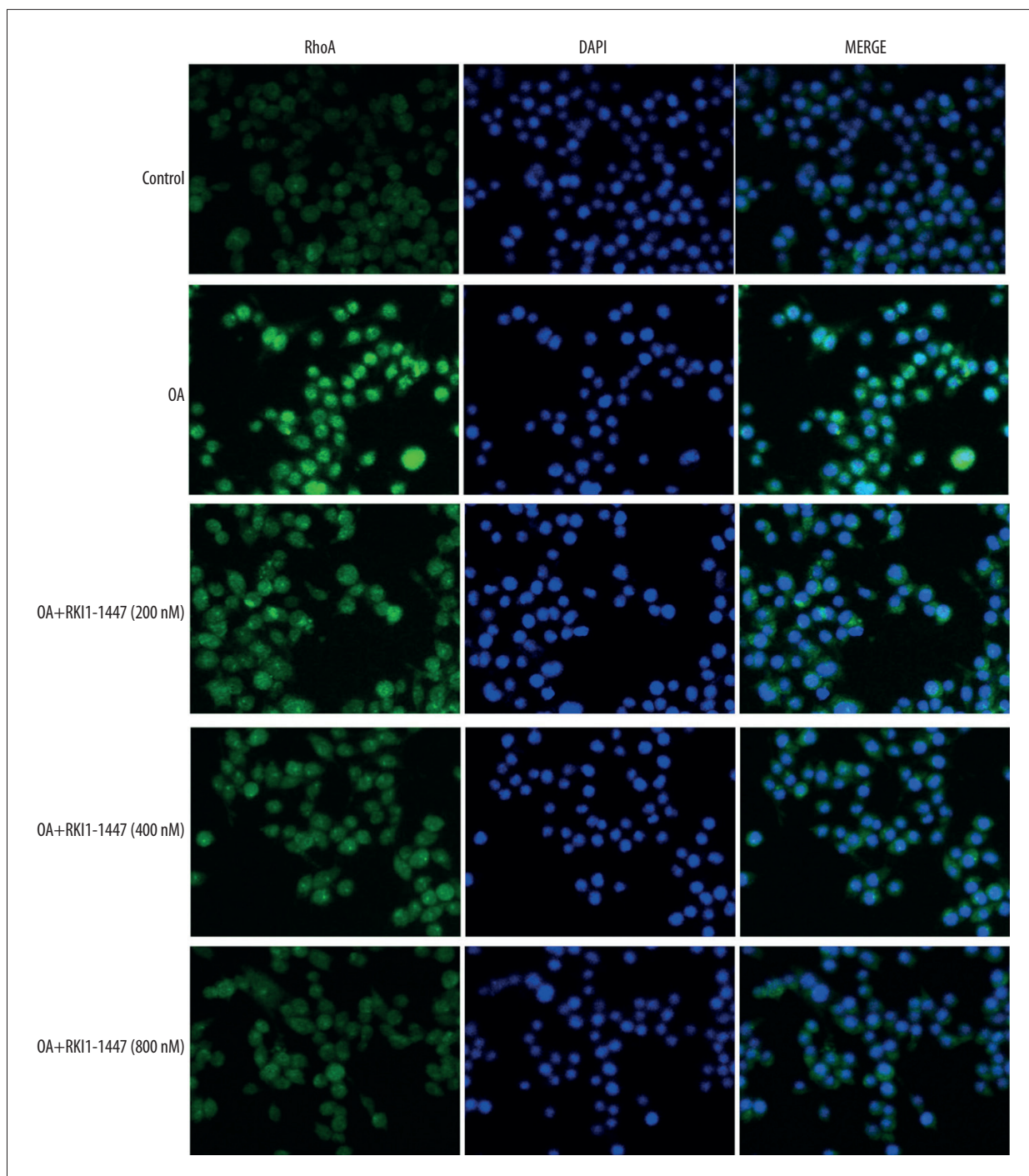


Figure 12. The effects of RKI-1447 on the RhoA expression of oleic acid-treated HepG2 human hepatocellular carcinoma cells. HepG2 cells were treated with or without the ROCK inhibitor RKI-1447 (200 nM, 400 nM, 800 nM) for 2 h. The cells were treated with oleic acid for 24 h and harvested.

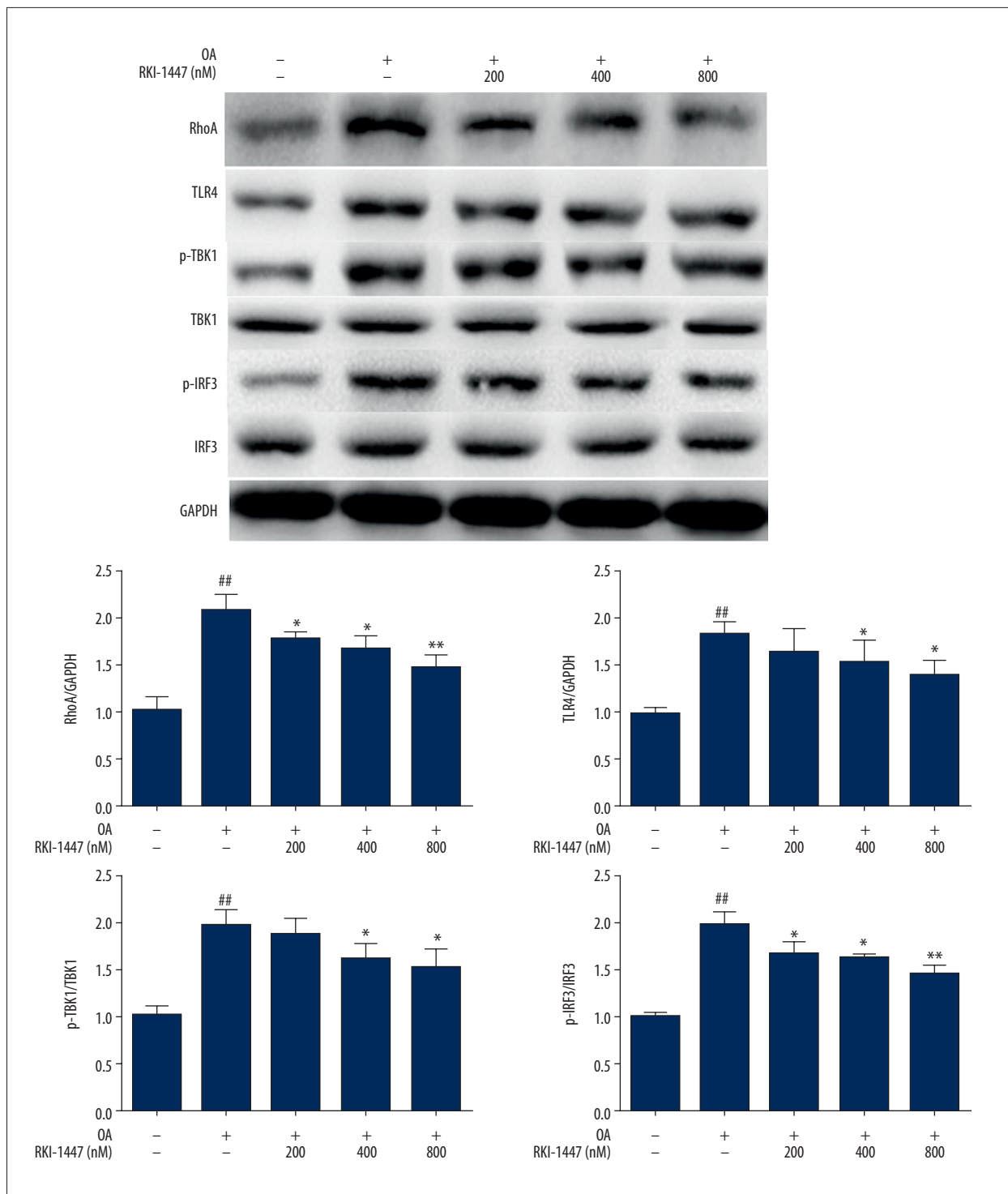


Figure 13. The effects of RKI-1447 on the ROCK/TLR4/TBK1/IRF3 pathway in oleic acid-treated HepG2 human hepatocellular carcinoma cells. HepG2 cells were treated with or without ROCK inhibitor RKI-1447(200, 400, 800 nM) for 2 h. Then the cells were treated with oleic acid for 24 h and collected for detection. Data are expressed as the mean±SD. Compared with the control: ^{##} p<0.01, ^{###} p<0.001. Compared with mice fed a high-fat diet. * p<0.05, ** p<0.01.

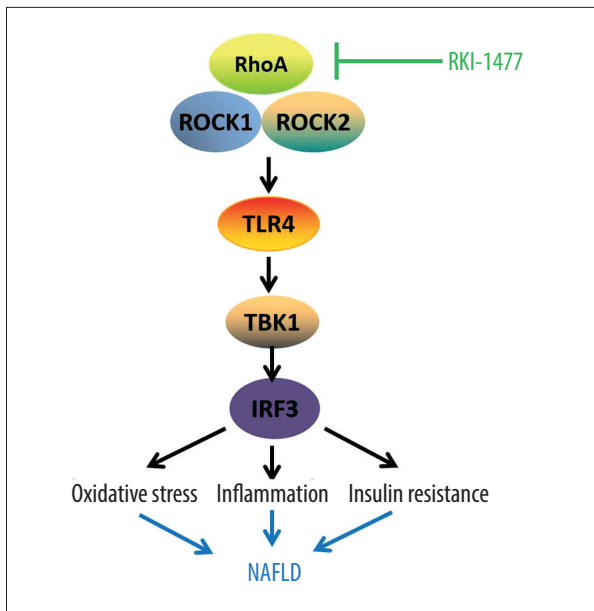


Figure 14. Diagram of the role of RKI-1447 in liver cells and the TLR4/TBK1/IRF3 signaling pathway.

It is possible that RKI-1447 exerted a protective role in liver cells via the TLR4/TBK1/IRF3 signaling pathway, as shown in Figure 14. In the present study, treatment with RKI-1447 significantly inhibited the expression of TLR4 and the phosphorylation of TBK1 and IRF3, both *in vivo* and *in vitro*.

Conclusions

This study aimed to investigate the effects of RKI-1447, a selective inhibitor of Rho-associated ROCK kinases, in a mouse model of nonalcoholic fatty liver disease (NAFLD) induced by a high-fat diet and in oleic acid-treated HepG2 human hepatocellular carcinoma cells *in vitro*. The findings showed that the inhibition of ROCK by RKI-1447 reduced the liver changes in a mouse model of NAFLD induced by a high-fat diet and in oleic acid-treated HepG2 cells by inhibiting inflammation, oxidative stress, and insulin resistance, possibly through the ROCK/TLR4/TBK1/IRF3 signaling pathway. These preliminary findings support the need for further *in vitro* and *in vivo* studies on the role of RKI-1447 in NAFLD.

References:

- Lenze EJ, Mulsant BH, Blumberger DM et al: Efficacy, safety, and tolerability of augmentation pharmacotherapy with aripiprazole for treatment-resistant depression in late life: A randomised, double-blind, placebo-controlled trial. *Lancet*, 2015; 386(10011): 2404–12
- Sherif ZA, Saeed A, Ghavimi S et al: Global epidemiology of nonalcoholic fatty liver disease and perspectives on US minority populations. *Dig Dis Sci*, 2016; 61(5): 1214–25
- Başaranoğlu M, Örmeci N: Nonalcoholic fatty liver disease: Diagnosis, pathogenesis, and management. *Turk J Gastroenterol*, 2014; 25(2): 127–32
- Kühn T, Nonnenmacher T, Sookthai D et al: Anthropometric and blood parameters for the prediction of NAFLD among overweight and obese adults. *BMC Gastroenterol*, 2018; 18(1): 113
- Simon TG, Trejo MEP, McClelland R et al: Circulating Interleukin-6 is a biomarker for coronary atherosclerosis in nonalcoholic fatty liver disease: Results from the Multi-Ethnic Study of Atherosclerosis. *Int J Cardiol*, 2018; 259: 198–204
- Tang X, Guo D, Lin C et al: hCLOCK causes Rho-kinase-mediated endothelial dysfunction and NF- κ B-mediated inflammatory responses. *Oxid Med Cell Longev*, 2015; 2015: 671839
- Feng G, Sun B, Liu HX et al: EphA2 antagonism alleviates LPS-induced acute lung injury via Nrf2/HO-1, TLR4/MyD88 and RhoA/ROCK pathways. *Int Immunopharmacol*, 2019; 72: 176–85
- Tsukamoto H, Takeuchi S, Kubota K et al: Lipopolysaccharide (LPS)-binding protein stimulates CD14-dependent Toll-like receptor 4 internalization and LPS-induced TBK1-IK κ -IRF3 axis activation. *J Biol Chem*, 2018; 293(26): 10186–201
- Kumari M, Wang X, Lantier L et al: IRF3 promotes adipose inflammation and insulin resistance and represses browning. *J Clin Invest*, 2016; 126(8): 2839–45
- Qiao JT, Cui C, Qing L et al: Activation of the STING-IRF3 pathway promotes hepatocyte inflammation, apoptosis and induces metabolic disorders in nonalcoholic fatty liver disease. *Metabolism*, 2018; 81: 13–24
- Trebicka J, Von HM, Lehmann J et al: Assessment of response to beta-blockers by expression of β Arr2 and RhoA/ROCK2 in antrum mucosa in cirrhotic patients. *J Hepatol*, 2016; 64(6): 1265–73
- Wong CM, Wei L, Au SL et al: MiR-200b/200c/429 subfamily negatively regulates Rho/ROCK signaling pathway to suppress hepatocellular carcinoma metastasis. *Oncotarget*, 2015; 6(15): 13658–70
- Sun X, Zhu Y, Wang QE et al: Su1849 involvement of protein kinase A and RhoA/ROCK pathway in diabetic colonic dysmotility. *Gastroenterol*, 2015; 148(4): S-532–33
- Patel RA, Forinash KD, Roberta P et al: RKI-1447 is a potent inhibitor of the Rho-associated ROCK kinases with anti-invasive and antitumor activities in breast cancer. *Cancer Res*, 2012; 72(19): 5025–34
- Zhao J, Zheng H, Liu Y et al: Anti-inflammatory effects of total alkaloids from *Rubus alceifolius* Poir [corrected], on non-alcoholic fatty liver disease through regulation of the NF- κ B pathway. *Int J Mol Med*, 2013; 31(4): 931–37
- Daneshi-Maskooni M, Keshavarz SA, Mansouri S et al: The effects of green cardamom on blood glucose indices, lipids, inflammatory factors, paraxonase-1, sirtuin-1, and irisin in patients with nonalcoholic fatty liver disease and obesity: Study protocol for a randomized controlled trial. *Trials*, 2017; 18(1): 260
- Chen S, Kang Y, Sun Y et al: Deletion of Gab2 in mice protects against hepatic steatosis and steatohepatitis: A novel therapeutic target for fatty liver disease. *J Mol Cell Biol*, 2016; 8(6): 492
- Zhang Y, Cui Y, Wang XL et al: PPAR α / γ agonists and antagonists differentially affect hepatic lipid metabolism, oxidative stress and inflammatory cytokine production in steatohepatic rats. *Cytokine*, 2015; 75(1): 127–35
- Xu M, Zheng XM, Jiang F, Qiu WQ: MicroRNA-190b regulates lipid metabolism and insulin sensitivity by targeting IGF-1 and ADAMTS9 in non-alcoholic fatty liver disease. *J Cell Biochem*, 2018; 119(7): 5864–74
- Song L, Qu D, Zhang Q et al: Phytosterol esters attenuate hepatic steatosis in rats with non-alcoholic fatty liver disease rats fed a high-fat diet. *Sci Rep*, 2017; 7: 41604
- Chong L, Laight D, Fowell AJ et al: PWE-133 Vascular inflammation is associated with endothelial dysfunction and oxidative stress in patients with non-alcoholic fatty liver disease. *Gut*, 2015; 64: A271–72
- Kammoun HL, Allen TL, Henstridge DC et al: Over-expressing the soluble gp130-Fc does not ameliorate methionine and choline deficient diet-induced non alcoholic steatohepatitis in mice. *PLoS One*, 2017; 12(6): e0179099
- Peng CH, Lin HT, Chung DJ et al: Mulberry Leaf Extracts prevent obesity-induced NAFLD with regulating adipocytokines, inflammation and oxidative stress. *J Food Drug Anal*, 2018; 26(2): 778–87
- Abdali NT, Yaseen AH, Said E, Ibrahim TM: Rho kinase inhibitor fasudil mitigates high-cholesterol diet-induced hypercholesterolemia and vascular damage. *Naunyn Schmiedebergs Arch Pharmacol*, 2017; 390(4): 409–22

25. Stanimirovic J, Obradovic M, Panic A et al: Regulation of hepatic Na⁺/K⁺-ATPase in obese female and male rats: involvement of ERK1/2, AMPK, and Rho/ROCK. *Mol Cell Biochem*, 2017; 440(11): 1–12
26. Soliman H, Nyamandi V, Garciapatino M et al: Partial deletion of ROCK2 protects mice from high-fat diet-induced cardiac insulin resistance and contractile dysfunction. *Am J Physiol Heart Circ Physiol*, 2015; 309(1): H70
27. Hu X, Yu D, Zhuang L et al: Geniposide improves hepatic inflammation in diabetic db/db mice. *Int Immunopharmacol*, 2018; 59: 141–47
28. Wong CC, Wong CM, Tung EK et al: Rho-kinase 2 is frequently overexpressed in hepatocellular carcinoma and involved in tumor invasion. *Hepatology*, 2010; 49(5): 1583–94
29. Xue W, Fan Z, Li Y et al: Alkannin Inhibited Hepatic Inflammation in Diabetic Db/Db Mice. *Cell Physiol Biochem*, 2018; 45(6): 2461–70
30. Lu L, Yue S, Jiang L et al: Myeloid Notch1 deficiency activates RhoA/ROCK pathway and aggravates hepatocellular damage in mouse ischemic livers. *Hepatology*, 2018; 67(3): 1041–55
31. Hutchinson JL, Rajagopal SP, Mei Y, Norman JE: Lipopolysaccharide promotes contraction of uterine myocytes via activation of Rho/ROCK signaling pathways. *FASEB J*, 2014; 28(1): 94–105
32. Wang Q, Cheng F, Xu Y et al: Thymol alleviates lipopolysaccharide-stimulated inflammatory response via downregulation of RhoA-mediated NF-kappaB signalling pathway in human peritoneal mesothelial cells. *Eur J Pharmacol*, 2018; 833: 210–20
33. Wei S, Zhou H, Wang Q et al: RIP3 deficiency alleviates liver fibrosis by inhibiting ROCK1-TLR4-NF-kappaB pathway in macrophages. *FASEB J*, 2019; 33(10): 11180–93
34. Hutchinson JL, Rajagopal SP, Yuan M, Norman JE: Lipopolysaccharide promotes contraction of uterine myocytes via activation of Rho/ROCK signaling pathways. *FASEB J*, 2014; 28(1): 94–105
35. Zhai Y, Shen XD, Gao F et al: CXCL10 regulates liver innate immune response against ischemia and reperfusion injury. *Hepatology*, 2010; 47(1): 207–14
36. Black KE, Collins SL, Hagan RS et al: Hyaluronan fragments induce IFN β via a novel TLR4-TRIF-TBK1-IRF3-dependent pathway. *J Inflamm*, 2013; 10(1): 23
37. Shi Y, Du L, Lv D et al: Exosomal interferon-induced transmembrane protein 2 transmitted to dendritic cells inhibits interferon alpha pathway activation and blocks anti-hepatitis B virus efficacy of exogenous interferon alpha. *Hepatology*, 2019; 69(6): 2396–413
38. Xin-An W, Ran Z, Zhi-Gang S et al: Interferon regulatory factor 3 constrains IKK β /NF- κ B signaling to alleviate hepatic steatosis and insulin resistance. *Hepatology*, 2014; 59(3): 870–85
39. Xie W, Lv A, Li R et al: *Agaricus blazei* murill polysaccharides protect against cadmium-induced oxidative stress and inflammatory damage in chicken spleens. *Biol Trace Elem Res*, 2017; 184(1): 1–12